Spectrochimica Acta Part A: Molecular and Biomolecular Spectroscopy 281 (2022) 121580

Contents lists available at ScienceDirect

Spectrochimica Acta Part A:
Molecular and Biomolecular Spectroscopy

journal homepage: www.journals.elsevier.com/spectrochimica-acta-part-a-molecular-and-biomolecular-spectroscopy

Preparation and SERS performance of silver nanowires arrays on paper by automatic writing method

Kun Wang, Zhiyu Qiu, Yufei Qin, Longxiu Feng, Lei Huang, Guina Xiao *

Department of Physics, Shanghai Normal University, Guilin Road 100, Shanghai 200234, PR China

HIGHLIGHTS

- Silver nanowires arrays were prepared by automatic writing method.
- The detection limit of crystal violet adsorbed on the arrays was down to 10^{-15} mol/L.
- The arrays exhibited good uniformity and repeatability with RSD of about 10%.
- Crystal violet residue was successfully detected by continuously pressing nine times.
- The quantitative analyses of 2, 2′-bipyridyl were achieved based on the arrays.

GRAPHICAL ABSTRACT

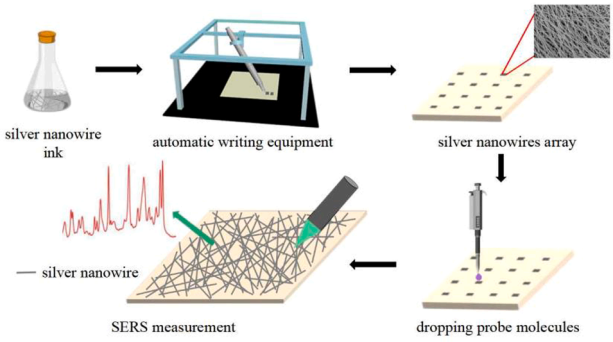

ARTICLE INFO

Keywords:
Silver nanowires
SERS
Crystal violet
Automatic writing method
2, 2′-bipyridyl

ABSTRACT

Silver nanowire ink was written on the surface of drawing paper by automatic writing method. Scanning electron microscopy was used to characterize the surface morphologies of the drawing paper before and after writing silver nanowires. The effects of fabrication parameters and measurement parameters on silver nanowires arrays were investigated. Crystal violet was selected as the probe molecule to study the SERS performance of silver nanowires arrays. The detection limit of crystal violet was as low as 10^{-15} mol/L. The uniformity and repeatability of the arrays were also explored, and the relative standard deviation values were about 10%. Moreover, silver nanowires arrays were also relatively stable that SERS signals were still observed after ten weeks. Detection of the crystal violet residue was further achieved on the substrates by continuously pressing nine times. In addition, silver nanowires arrays were also applied to the quantitative analyses of 2, 2′-bipyridyl.

1. Introduction

Surface-enhanced Raman scattering (SERS) is a nondestructive, highly sensitive and selective analysis technique, which plays an important role in food detection, environmental monitoring and pharmaceutical analyses [1–4]. There are two main enhancement mechanisms of SERS: electromagnetic enhancement and chemical enhancement [5,6]. It is generally believed that the electromagnetic enhancement excited by surface plasmon resonance contributes to the enhancement of the weak Raman scattering from target molecules [7].

* Corresponding author.
E-mail address: xiaoguina@shnu.edu.cn (G. Xiao).

https://doi.org/10.1016/j.saa.2022.121580
Received 8 May 2022; Received in revised form 15 June 2022; Accepted 29 June 2022
Available online 3 July 2022

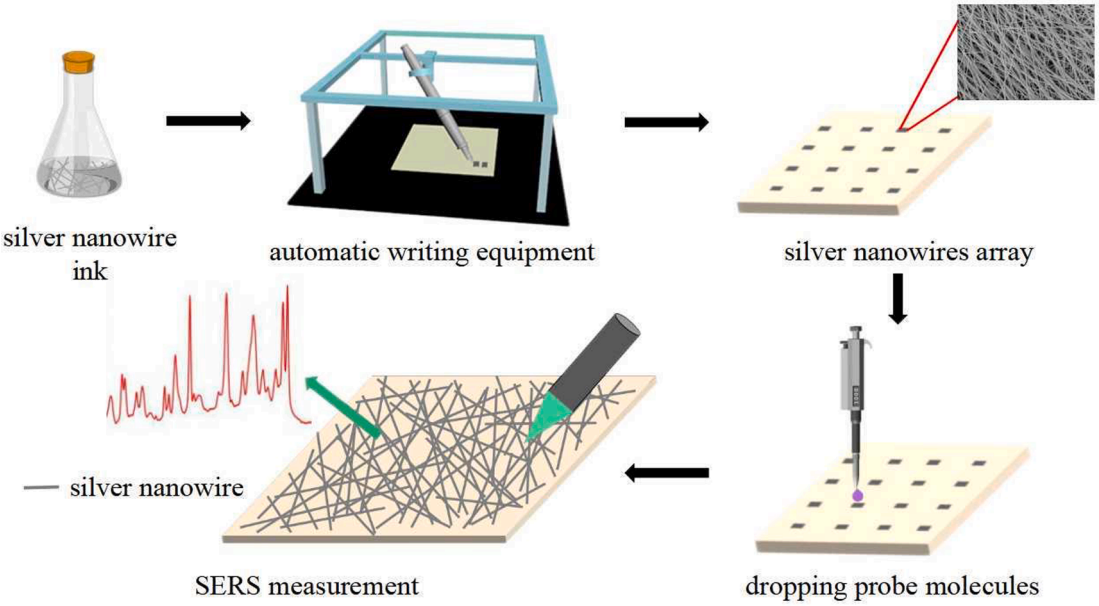

Fig. 1. Schematic diagram of the preparation and detection of silver nanowires array.

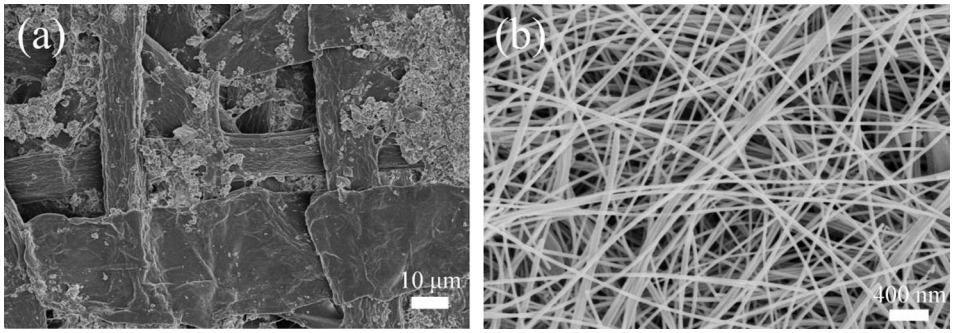

Fig. 2. SEM images of drawing paper (a) uncoated and (b) coated with silver nanowires.

The electromagnetic field around the nanostructures is often called "hot spots". Hot spots are mainly determined by the size of nanostructures [8], period of nanostructure arrays [9] or the nanoscale gap between two nanostructures [10]. Chemical enhancement is concerned with charge transfer interactions between substrates and target molecules [11]. Silver is considered to be the best SERS material with a strong signal response [12]. Silver nanostructures with various shapes, including nanoparticles, nanowires, nanorods, nanoplates and so on have been prepared [13–16]. Among them, nanostructures with high curvature surfaces and sharp edges exhibited great Raman scattering enhancement [17,18]. Silver nanowires possess non-circular cross-section and tip properties, which are conducive to the effective enrichment of local electromagnetic fields [19,20]. Previous studies have shown that the nanotips and particle gaps of silver nanowires tended to generate strong hot spots, which was very beneficial for the detection of target molecules [21,22].

Paper is widely used as a supporting base for SERS substrates due to its lightness, flexibility and low cost [23]. Additionally, the hierarchical roughness of paper provides greater surface area for analytes detection [24]. At present, several different methods have been employed to prepare SERS substrates on paper, such as screen printing, inkjet printing, dropping method [19,25,26]. For example, Joshi et al. prepared silver nanowires paper-based SERS substrates on demand by inkjet printing silver halide, and the substrates could be preserved for one year under environmental conditions [25]. Sun et al. directly dropped silver nanowires on the surface-modified paper to prepare a paper-based SERS substrate and successfully detected furazolidone in different environments [19]. These substrates have shown great potential as low cost, disposable and reproducible for molecular analyses. However, there is still a need to improve the reproducibility and reduce the cost of preparing SERS substrates. Automatic writing is a machine that mimics human handwriting. At present, automatic writing technique has been used in the fields of human health monitoring and electronic sensors [27,28]. Automatic writing machine can adjust writing speed and design required patterns. Moreover, the operation process of automatic writing instrument is simple and safe.

In this paper, silver nanowires arrays were prepared on drawing paper by automatic writing method. Firstly, the optimal preparation and measurement parameters affecting the SERS performance of silver nanowires arrays were studied. Subsequently, the SERS activities of silver nanowires arrays were evaluated using crystal violet. And the uniformity, repeatability and stability of the arrays were further explored. Moreover, the arrays were used for SERS detection of crystal violet residues in consecutive nine fingerprints and quantitative analyses of 2, 2′-bipyridyl.

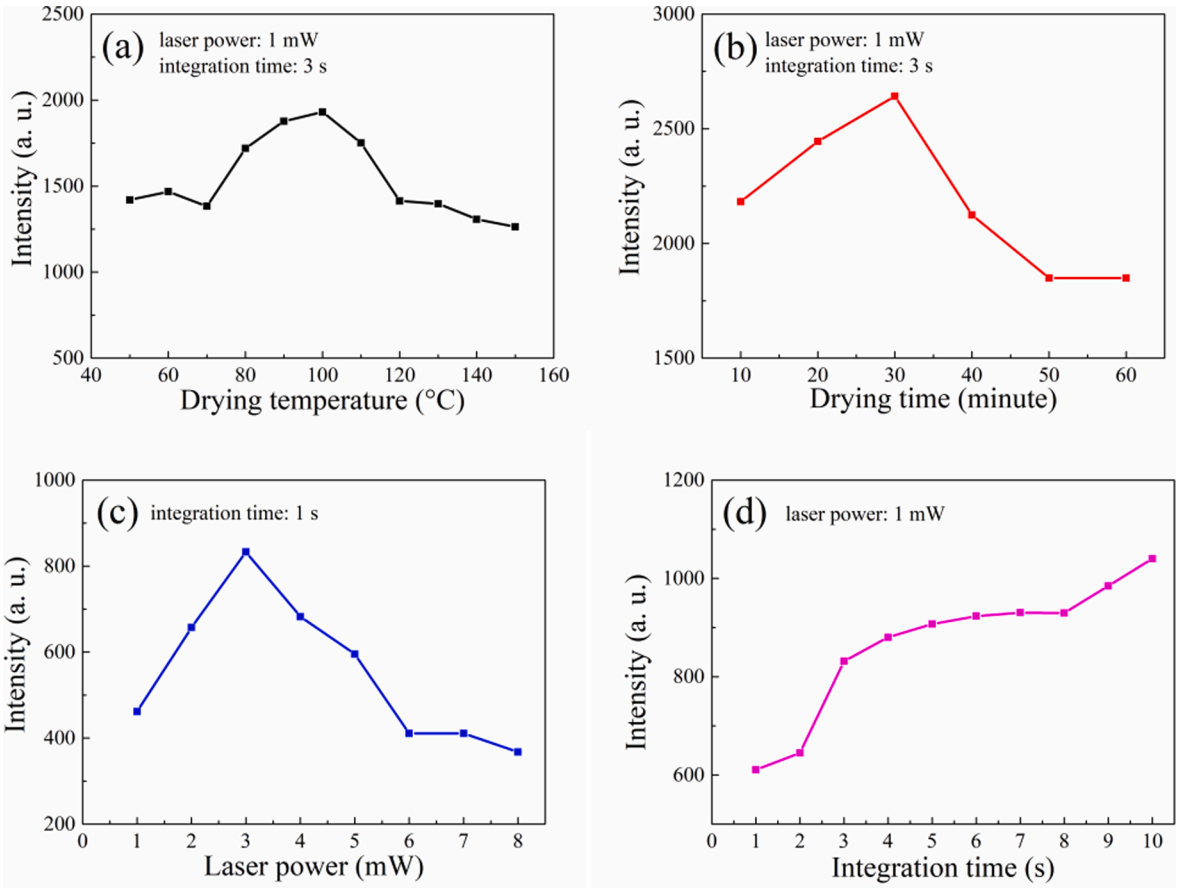

Fig. 3. The plots of different (a) drying temperatures, (b) drying time, (c) laser powers and (d) integration time versus the peak intensities of crystal violet adsorbed on silver nanowires arrays.

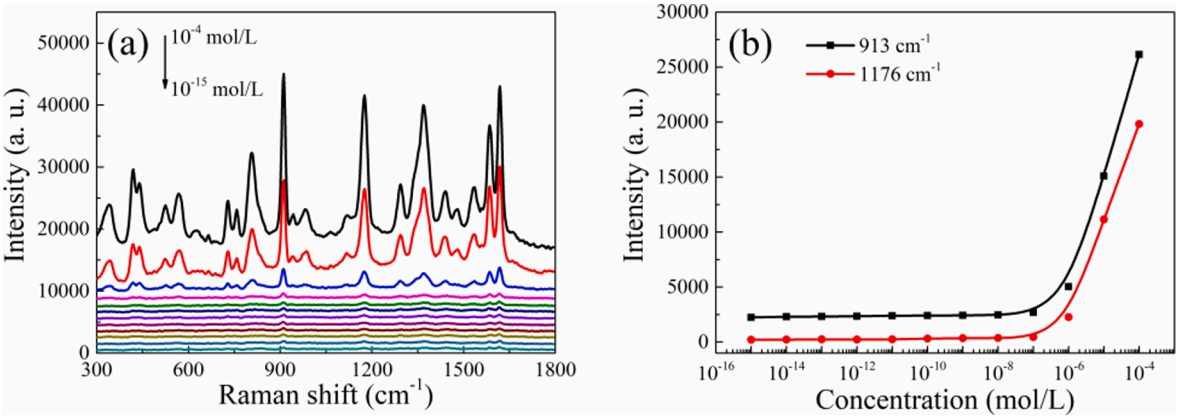

Fig. 4. (a) SERS spectra of crystal violet with different concentrations absorbed on silver nanowires arrays. (b) The relationship between crystal violet concentrations and peak intensities at 913 and 1176 cm^{-1}.

Table 1
Silver nanowires SERS substrates prepared by different methods.

SERS substrates	Methods	Supporting materials	Probe molecules	Limit of detection (LOD)	References
AgNWs@AgNPs film	Interface self-assembly	Shape memory polyurethane (SMPU)	Rhodamine B	10^{-10} mol/L	[33]
AgNWs paper substrate	Dropping	Filter paper	Methylene blue (MB)	10^{-8} mol/L	[19]
AgNWs-network-film (AgNWNF)	Spraying	Polydimethyl siloxane (PDMS)	Rhodamine 6G (R6G)	10^{-7} mol/L	[34]
AgNWs film	Evaporation-induced aggregation	Glass slide	Rhodamine 6G (R6G)	10^{-10} mol/L	[35]
AgNWs@PDMS	Dropping	Polydimethyl siloxane (PDMS)	Malachite green (MG)	10^{-8} mol/L	[36]
AgNWs arrays	Automatic writing	Drawing paper	Crystal violet (CV)	10^{-15} mol/L	This work

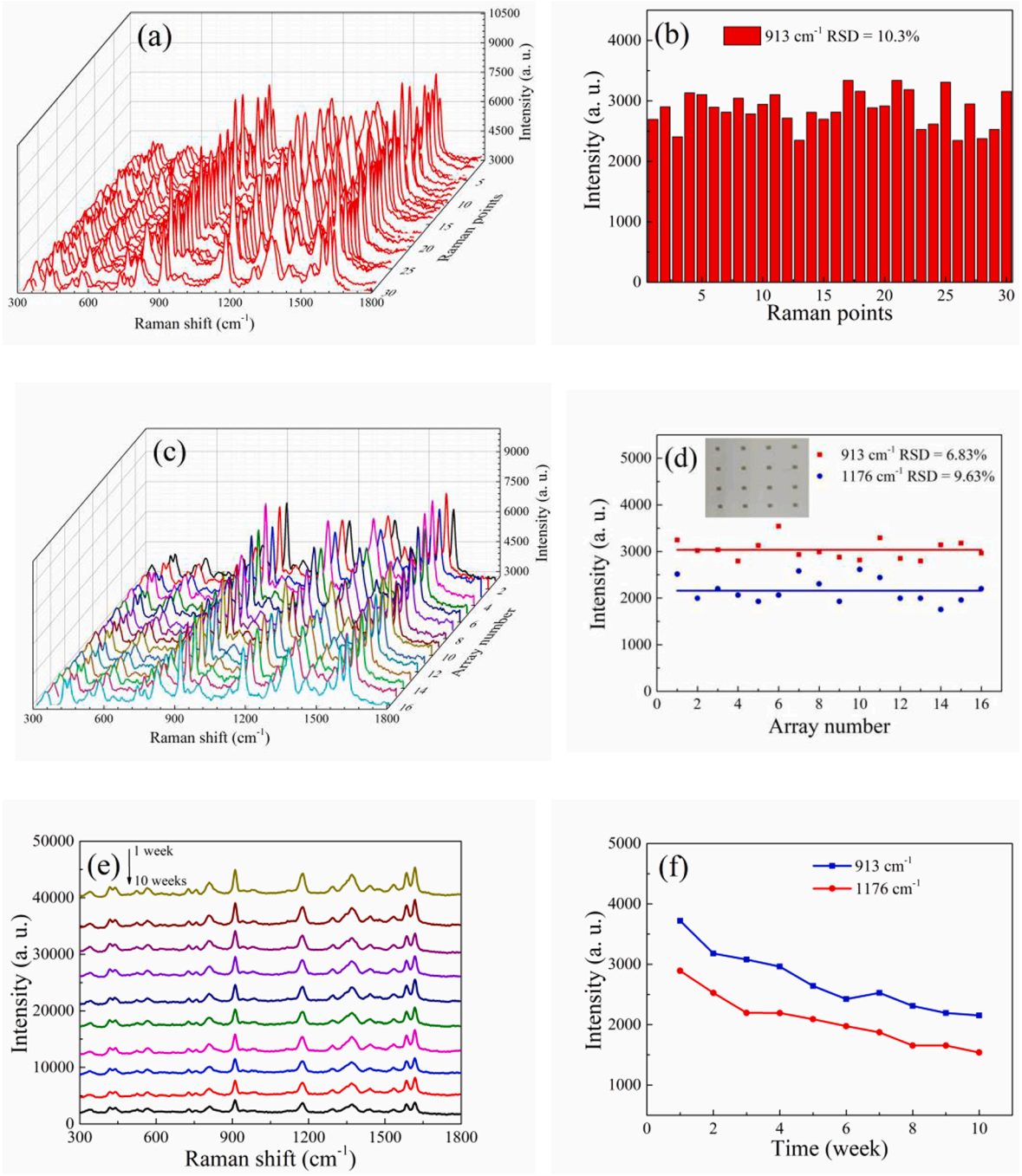

Fig. 5. (a) SERS spectra of thirty points of crystal violet adsorbed on the same array and (b) the corresponding SERS intensity distribution at 913 cm^{-1}. (c) SERS spectra of crystal violet obtained from 4 × 4 silver nanowires arrays and (d) the corresponding SERS intensities at 913 and 1176 cm^{-1}. (e) SERS spectra of crystal violet during different storage time and (f) the corresponding SERS intensities at 913 and 1176 cm^{-1}.

2. Experimental

2.1. Materials and reagents

Silver nanowire ink with diameters and length of 30 ~ 60 nm and 10 ~ 50 μm was purchased from Zhejiang Kechuang Advanced Materials Technology Co., Ltd.. The drawing paper (9.15 g/piece, white color, Guangbo Group Co., Ltd.) was purchased from the local supermarket. The paper did not require special treatment before writing. The pen with a tip of 0.7 mm was bought from Shanghai Boccaccio Industry Co., Ltd.. Table S1 exhibited the details of the pen. The automatic writing device was supplied by Hunan Chuanglebo Intelligent Technology Co., Ltd. (Hunan, China). The characteristic parameters of automatic writing device were exhibited in Table S2. Crystal violet and 2, 2′-bipyridyl were provided by Shanghai Bailingwei Chemical Technology Co., Ltd. and Shanghai Maclin Biochemical Technology Co., Ltd., respectively. The specific chemical structural structures of crystal violet and 2, 2′-bipyridyl were shown in Fig. S1. Concentrated hydrochloric acid (HCl, 36–38 wt%) was supplied by Shanghai Runjie Chemical Reagent Co., Ltd.. Crystal violet ethanol solution with a concentration of 10^{-2} mol/L was prepared. Then the stock solution was diluted with deionized water to prepare crystal violet solutions with concentrations from 10^{-3} to 10^{-15} mol/L.

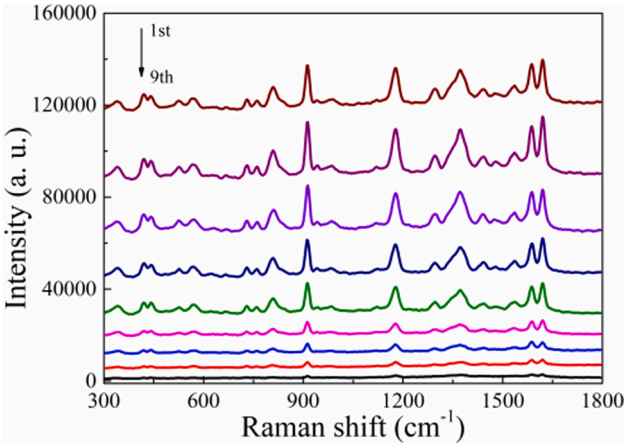

Fig. 6. SERS spectra of crystal violet were obtained by pressing the fingerprint on silver nanowires arrays.

2.2. Preparation of silver nanowires arrays on drawing paper

Fig. 1 showed the schematic diagram of fabricating silver nanowires arrays by automatic writing method. Firstly, silver nanowire ink was filled into a pen and the pen was fixed in the card slot of the automatic writing device. Parameters such as the shape and size of the substrate, the writing speed and height of the device were set through the computer connected to the automatic writing device. In the experiment, the shape of the substrate was set as a square of 2 × 2 mm^2, and the writing speed and height of the instrument were 5000 mm/min and 3 mm, respectively. Secondly, the silver nanowires arrays were dried in an oven with different drying temperatures and drying time, respectively. Finally, crystal violet solutions with different concentrations were dropped onto the silver nanowires arrays. After evaporation, the SERS spectra were collected by Raman spectrometer.

2.3. Characterization

The surface morphology of the drawing paper before and after writing silver nanowire ink were characterized by field emission scanning electron microscopy (S4800, SEM, Hitachi) at an accelerating voltage of 5.0 kV. Normal Raman spectra and SERS spectra were measured using the PTT-MRI Raman spectrometer (ProTrusTech Co., Ltd.) equipped with a 532 nm laser. The SERS spectra were measured from 300 to 1800 cm^{-1}. The accumulated time and the resolution were one time and 2 cm^{-1}, respectively. The laser power incident on the sample was 3 mW and the integration time was 3 s. For 2, 2′-bipyridyl, the laser power on the sample was 5 mW, and each spectrum was collected with the integration time of 10 s.

3. Results and discussion

3.1. Morphological characterization of silver nanowires arrays

Fig. 2(a) exhibited a low-magnification SEM image of the drawing paper. Note that besides the naturally folded three-dimensional structure, some particulates were also observed. These particulates are presumed to be pigment fillers, which are used in the manufacture of office paper [29]. The SEM image of the drawing paper coated with silver nanowires was presented in Fig. 2(b). It can be seen that silver nanowires were interwoven to form network structures. The cross sectional SEM images of silver nanowires on drawing paper at different magnifications were shown in Fig. S2. The thickness of the silver nanowires was about 3.34 μm. The SERS intensity was mainly concentrated in the gaps between adjacent nanowires and in the nanowire tips to form “hot spots”.

3.2. The effect of preparation and test parameters on SERS activities of silver nanowires arrays

The SERS spectra of crystal violet adsorbed on different paper-based silver nanowires arrays were exhibited in Fig. S3. By comparison, it could be found that the silver nanowires arrays on drawing paper had relatively high SERS intensity. Therefore, the following research mainly discussed the silver nanowires arrays on drawing paper. During the preparation of the arrays, drying temperature and time were the important parameters. To investigate the effect of drying temperature on SERS activities of the arrays, SERS spectra of crystal violet adsorbed on the arrays dried from 50 to 150 °C were collected. The laser power and integration time were 1 mW and 3 s, respectively. The characteristic peak at 913 cm^{-1} was picked to calculate the peak intensity. And the relationship between drying temperature and SERS intensity was plotted in Fig. 3(a). The peak intensity first increased and then decreased gradually with the increase of drying temperature. The best performance was achieved when the drying temperature reached 100 °C. Fig. 3(b) displayed the relationship between different drying time and SERS activities of silver nanowires arrays under the same measurement conditions. The silver nanowires adhered to the drawing paper better when the drying time was 30 min. In addition, laser power and integration time were also the important parameters. Fig. 3(c) showed the SERS activities of the arrays with laser power from 1 mW to 8 mW and integration time of 1 s. The SERS activities increased with laser power and the best performance was reached at 3 mW. However, the SERS activities gradually decreased with the further increase of laser power. The

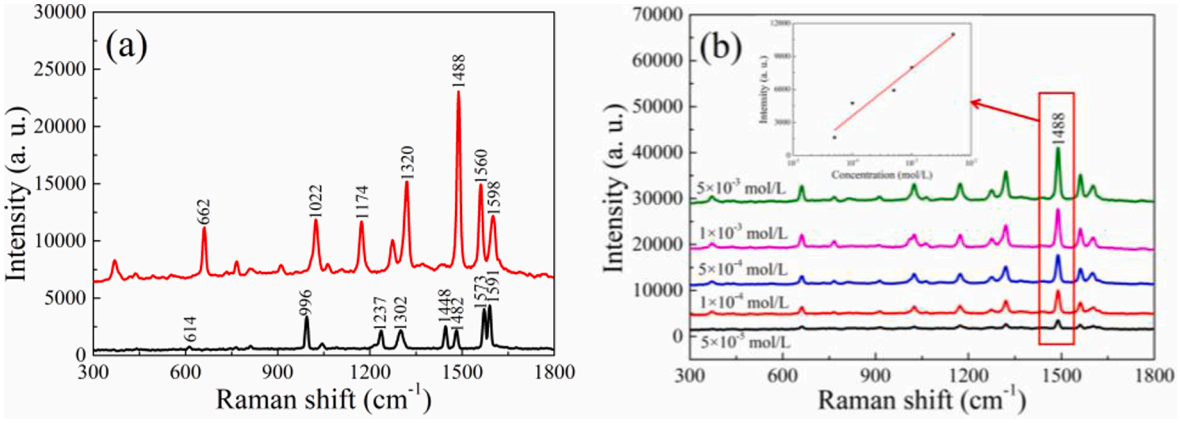

Fig. 7. (a) Normal Raman spectrum of 2, 2′-bipyridyl solid powder (black line) and SERS spectrum of 10^{-3} mol/L 2, 2′-bipyridyl after dropping HCl (red line). (b) SERS spectra of 2, 2′-bipyridyl with different concentrations after dropping HCl and the peak intensity at 1488 cm^{-1} versus 2, 2′-bipyridyl concentration.

excess laser power would burn the arrays and reduce the SERS activities. When the laser power is 1 mW, the line graph of different integration time versus the peak intensity of crystal violet was presented in Fig. 3(d). The peak intensity increased with integration time. To achieve fast and sensitive SERS detection, the laser power and integration time were selected as 3 mW and 3 s in the following experiments.

3.3. SERS sensitivity of silver nanowires arrays

To further evaluate its SERS sensitivity, the SERS spectra of crystal violet with different concentrations were measured under the same condition as depicted in Fig. 4(a). The characteristic peaks at 913, 1176, 1372 and 1620 cm^{-1} were clearly distinguished. Among them, the peak at 913 cm^{-1} could be attributed to ring skeletal vibration. The peak at 1176 cm^{-1} corresponded to the characteristic of C − H in plane bending vibrations. The peaks at 1372 and 1620 cm^{-1} represented N-phenyl stretching and ring C − C stretching, respectively [30–32]. Fig. 4(b) visually depicted the relationship between the concentrations of crystal violet and the SERS intensities at 913 and 1176 cm^{-1}. The SERS intensities continuously decreased with the decrease of crystal violet solution concentration. However, the SERS intensities did not change significantly after the concentration was reduced to 10^{-8} mol/L, and two main characteristic peaks could still be observed. The minimum detection concentration of crystal violet is 10^{-15} mol/L. The results indicated that the silver nanowires arrays had strong SERS responses. Table 1 listed the detection performance of silver nanowires SERS substrates prepared by different methods. The arrays prepared by the automatic writing method showed better sensitivity compared with silver nanowires SERS substrates reported in other literatures [19,33–36].

3.4. SERS properties of silver nanowires arrays

The uniformity, reproducibility and stability of silver nanowires arrays were systematically investigated. To study the uniformity of the arrays, thirty points were randomly selected on the same silver nanowires array. The SERS spectra were displayed in Fig. 5(a), and each spectral line was nearly identical. Furthermore, the peak intensities at 913 cm^{-1} were plotted as a bar graph in Fig. 5(b). The relative standard deviation (RSD) value was calculated to be 10.3%. Therefore, the prepared silver nanowires arrays can serve as a relatively reliable SERS detection platform.

In order to further explore the reproducibility of arrays, 4 × 4 silver nanowires arrays were prepared on the drawing paper by automatic writing method. The photograph of silver nanowires arrays was shown in the inset of Fig. 5(d). The SERS spectra of crystal violet obtained from the silver nanowires arrays were presented in Fig. 5(c). The sixteen spectral lines could be well overlapped after being shifted. Fig. 5(d) displayed a scatter plot of SERS intensity variations corresponding to the peaks at 913 and 1176 cm^{-1}. The corresponding RSD values were 6.83% and 9.63%, respectively, which indicated that the prepared silver nanowires arrays had good reproducibility.

Silver is easily oxidized during long-term storage. Therefore, the stability during storage is critical for the practicality of the SERS arrays. To study the stability, the SERS spectra of crystal violet were collected from the same array every week at room temperature, as shown in Fig. 5(e). The SERS signals can be detected even if the array was preserved for ten weeks. Each spectral line had good resolution and the peak positions were almost identical. Fig. 5(f) exhibited the SERS intensities changes at 913 and 1176 cm^{-1} within ten weeks. The results indicated that the silver nanowires arrays were relatively stable at ambient temperature.

3.5. Fingerprint detection

Aromatic dyes can be used to enhance the visualization of fingerprints [36]. Therefore, the detection of crystal violet residues in fingerprints was explored based on the above-mentioned SERS arrays. A drop of 10^{-2} mol/L crystal violet solution (2.5 μL) was dropped on the finger and continuously pressed on the arrays for SERS detection. Fig. 6 showed the SERS spectra from the first to ninth pressing. It is evident that the Raman characteristic peaks of crystal violet were still clearly visible even after the ninth pressing.

3.6. Quantitative analyses of 2, 2′-bipyridyl

2, 2′-bipyridyl, an aromatic heterocyclic compound containing nitrogen, was selected to further detect the SERS performance of the arrays [37]. The SERS signals could not be detected by directly dropping 2, 2′-bipyridyl on the silver nanowires arrays. The reason may be that 2, 2′-bipyridyl molecules can't attach to silver nanowires. Therefore, it is necessary to find a substance to help 2, 2′-bipyridyl molecules adsorb on the surface of arrays. Chlorine ions in hydrochloric acid (HCl) can form Ag-Cl active sites with silver atoms that are conducive to molecular chemical adsorption and SERS enhancement, thereby enhancing the molecules signals [38,39]. Fig. 7(a) displayed the normal Raman spectrum of 2, 2′-bipyridyl solid powder and SERS spectrum of 10^{-3} mol/L 2, 2′-bipyridyl after dropping HCl. Compared with the normal Raman spectrum, the peak positions were slightly shifted. It may be caused by the interaction between 2, 2′-bipyridyl molecules and the arrays [40]. A series of 2, 2′-bipyridyl solutions with different concentrations were dropped on silver nanowires arrays. After they were completely dried, 3 μL of 0.1 mol/L HCl was dropped on the above arrays. The SERS spectra were then collected before the HCl evaporated, as shown in Fig. 7(b). The SERS signals decreased with decreasing the concentration of 2, 2′-bipyridyl. The laser power and the integration time were 5 mW and 10 s, respectively. Moreover, the detection limit of 2, 2′-bipyridyl was as low as 5×10^{-5} mol/L. The linear relationship between the SERS intensity at 1488 cm^{-1} and concentration was exhibited in the inset of Fig. 7(b).

4. Conclusion

In this paper, a simple, fast and mass-producible automatic writing method was adopted to fabricate silver nanowires SERS arrays. The method has the advantages of easy operation, high efficiency and automatic preparation. The prepared arrays exhibited strong SERS response to crystal violet and a low detection concentration of 10^{-15} mol/L was obtained. In addition, silver nanowires also had good uniformity across a single array and high repeatability between different arrays. More importantly, the Raman scattering signal of crystal violet could still be observed after ten weeks of storage on the same array. Finally, the detection of crystal violet residues in fingerprints and the quantitative analyses of 2, 2′-bipyridyl were successfully achieved based on the above prepared SERS arrays. The results indicated that the prepared silver nanowires arrays are a relatively sensitive and reliable detection platform.

Declaration of Competing Interest

The authors declare that they have no known competing financial interests or personal relationships that could have appeared to influence the work reported in this paper.

Acknowledgements

This research was supported by the Natural Science Foundation of Shanghai(No. 19ZR1437700, 21ZR1446400), the National Natural Science Foundation of China(No. 22175119) and the Program of Shanghai Normal University(No. SK202138).

Appendix A. Supplementary material

Supplementary data to this article can be found online at https://doi.org/10.1016/j.saa.2022.121580.

References

[1] H.Q. Liu, Y.N. He, K.Z. Cao, Flexible surface-enhanced Raman scattering substrates: A review on constructions, applications, and challenges, Adv. Mater. Interfaces 8 (21) (2021) 2100982, https://doi.org/10.1002/admi.202100982.

[2] C.L. Gou, X.L. Zeng, H. Du, L. Li, Y.F. Tian, X.D. Hou, L. Wu, Sensitive detection of trace 4-methylimidazole utilizing a derivatization reaction-based ratiometric surface-enhanced Raman scattering platform, Talanta 237 (2022) 122925, https://doi.org/10.1016/j.talanta.2021.122925.

[3] V. Sivaprakasam, M.B. Hart, Surface-enhanced Raman spectroscopy for environmental monitoring of aerosols, ACS Omega 6 (15) (2021) 10150–10159, https://doi.org/10.1021/acsomega.1c00207.

[4] J. Cailletaud, C. De Bleye, E. Dumont, P.Y. Sacre, L. Netchacovitch, Y. Gut, M. Boiret, Y.M. Ginot, P. Hubert, E. Ziemons, Critical review of surface-enhanced Raman spectroscopy applications in the pharmaceutical field, J Pharamceut. Biomed. 147 (2018) 458–472, https://doi.org/10.1016/j.jpba.2017.06.056.

[5] S.Y. Ding, J. Yi, J.F. Li, B. Ren, D.Y. Wu, R. Panneerselvam, Z.Q. Tian, Nanostructure-based plasmon-enhanced Raman spectroscopy for surface analysis of materials, Nat. Rev. Mater. 1 (2016) 16021, https://doi.org/10.1038/natrevmats.2016.21.

[6] X.X. Han, W. Ji, B. Zhao, Y. Ozaki, Semiconductor-enhanced Raman scattering: active nanomaterials and applications, Nanoscale 9 (15) (2017) 4847–4861.

[7] S.Y. Ding, E.M. You, Z.Q. Tian, M. Moskovits, Electromagnetic theories of surface-enhanced Raman spectroscopy, Chem. Soc. Rev. 46 (13) (2017) 4042–4076.

[8] X.W. Shi, J.F. Zou, X.J. Chen, H.Y. Zheng, Z.X. Jin, F.Z. Li, J.G. Piao, The effect of size on the surface enhanced Raman scattering property of SiO2@PDA@AgNP core-shell-satellite nanocomposite, Chem. Lett. 49 (5) (2020) 534–537, https://doi.org/10.1246/cl.200040.

[9] S.H. Wei, M.J. Zheng, Q. Xiang, H.L. Hu, H.G. Duan, Optimization of the particle density to maximize the SERS enhancement factor of periodic plasmonic nanostructure array, Opt. Express 24 (2016) 20613–20620, https://doi.org/10.1364/OE.24.020613.

[10] H.L. Liu, Z.L. Yang, L.Y. Meng, Y.D. Sun, J. Wang, L.B. Yang, J.H. Liu, Z.Q. Tian, Three-dimensional and time-ordered surface-enhanced Raman scattering hotspot matrix, J. Am. Chem. Soc. 136 (14) (2014) 5332–5341, https://doi.org/10.1021/ja501951v.

[11] L.X. Xia, M.D. Chen, X.M. Zhao, Z.L. Zhang, J.R. Xia, H.X. Xu, M.T. Sun, Visualized method of chemical enhancement mechanism on SERS and TERS, J. Raman Spectrosc. 45 (2014) 533–540, https://doi.org/10.1002/jrs.4504.

[12] C.Y. Liu, X.H. Xu, W.X. Hu, X. Yang, P.P. Zhou, G.Y. Qiu, W.C. Ye, Y.M. Li, C. Y. Jiang, Synthesis of clean cabbagelike (111) faceted silver crystals for efficient surface-enhanced Raman scattering sensing of papaverine, Anal. Chem. 90 (16) (2018) 9805–9812, https://doi.org/10.1021/acs.analchem.8b01735.

[13] T.W. Xu, X.Q. Wang, X. Zhang, Z.C. Bai, Compact Ag nanoparticles anchored on the surface of glass fiber filter paper for SERS applications, Appl. Phy. A-Mater. 128 (2022) 317, https://doi.org/10.1007/s00339-022-05459-3.

[14] C. Amicucci, C. D'Andrea, M. de Angelis, M. Banchelli, R. Pini, P. Matteini, Cost effective silver nanowire-decorated graphene paper for drop-on SERS biodetection, Nanomaterials 11 (2021) 1495, https://doi.org/10.3390/nano11061495.

[15] S.M. Zou, L.W. Ma, J.H. Li, Y.H. Liu, D.L. Zhao, Z.J. Zhang, Ag nanorods-based surface-enhanced Raman scattering: synthesis, quantitative analysis strategies, and applications, Front. Chem. 7 (2019) 376, https://doi.org/10.3389/fchem.2019.00376.

[16] X.J. Wang, C.H. Zhu, X.Y. Hu, Q.L. Xu, H.P. Zhao, G.W. Meng, Y. Lei, Highly sensitive surface-enhanced Raman scattering detection of organic pesticides based on Ag-nanoplate decorated graphene-sheets, Appl. Surf. Sci. 486 (2019) 405–410, https://doi.org/10.1016/j.apsusc.2019.05.008.

[17] M. Zannotti, A. Rossi, R. Giovannetti, SERS activity of silver nanosphere, triangular nanoplates, hexagonal nanoplates and quasi-spherical nanoparticles: effect of shape and morphology, Coatings 10 (2020) 288, https://doi.org/10.3390/coatings10030288.

[18] M.K. Oh, Y.S. Shin, C.L. Lee, R. De, H. Kang, N.E. Yu, B.H. Kim, J.H. Kim, J.K. Yang, Morphological and SERS properties of silver nanorod array films fabricated by oblique thermal evaporation at various substrate temperatures, Nanoscale Res. Lett. 10 (2015) 259, https://doi.org/10.1186/s11671-015-0962-8.

[19] H.M. Sun, X.T. Li, Z.Y. Hu, C.J. Gu, D. Chen, J. Wang, B. Li, T. Jiang, X.F. Zhou, Hydrophilic-hydrophobic silver nanowire-paper based SERS substrate for in-situ detection of furazolidone under various environments, Appl. Surf. Sci. 556 (2021) 149748, https://doi.org/10.1016/j.apsusc.2021.149748.

[20] W.G. Chen, H.Y. Shi, F. Wan, P.Y. Wang, Z.L. Gu, W.H. Li, L.A. Ke, Y.Z. Huang, Substrate influence on the polarization dependence of SERS in crossed metal nanowires, J. Mater. Chem. C 5 (28) (2017) 7028–7034.

[21] W. Wei, Y.X. Du, L.M. Zhang, Y. Yang, Y.F. Gao, Improving SERS hot spots for on-site pesticide detection by combining silver nanoparticles with nanowires, J. Mater. Chem. C 6 (32) (2018) 8793–8803.

[22] E.H. Koh, C. Mun, C. Kim, S.G. Park, E.J. Choi, S.H. Kim, J. Dang, J. Choo, J.W. Oh, D.H. Kim, H.S. Jung, M13 bacteriophage/silver nanowire surface-enhanced Raman scattering sensor for sensitive and selective pesticide detection, ACS Appl. Mater. Inter. 10 (12) (2018) 10388–10397, https://doi.org/10.1021/acsami.8b01470.

[23] C.C. Huang, C.Y. Cheng, Y.S. Lai, Y, S, Lai, Paper-based flexible surface enhanced Raman scattering platforms and their applications to food safety, Trends Food Sci. Tech. 100 (2020) 349–358, https://doi.org/10.1016/j.tifs.2020.04.019.

[24] Y.H. Ngo, D. Li, G.P. Simon, G. Garnier, Gold nanoparticle-paper as a three-dimensional surface enhanced Raman scattering substrate, Langmuir 28 (23) (2012) 8782–8790, https://doi.org/10.1021/la3012734.

[25] P. Joshi, V. Santhanam, Paper-based SERS active substrates on demand, RSC Adv. 6 (72) (2016) 68545–68552.

[26] L.L. Qu, Q.X. Song, Y.T. Li, M.P. Peng, D.W. Li, L.X. Chen, J.S. Fossey, Y.T. Long, Fabrication of bimetallic microfluidic surface-enhanced Raman scattering sensors on paper by screen printing, Anal. Chim. Acta 792 (2013) 96–192, https://doi.org/10.1016/j.aca.2013.07.017.

[27] Z.D. Li, H. Liu, X.C. He, F. Xu, F. Li, Pen-on-paper strategies for point-of-care testing of human health, Trac-trend, Anal. Chem. 108 (2018) 50–64, https://doi.org/10.1016/j.trac.2018.08.010.

[28] Z.D. Li, H. Liu, C. Ouyang, W.H. Wee, X.Y. Cui, T.J. Lu, B. Pingguan-Murphy, F. Li, F. Xu, Recent advances in pen-based writing electronics and their emerging applications, Adv. Funct. Mater. 26 (2) (2016) 165–180, https://doi.org/10.1002/adfm.201503405.

[29] N.C.T. Martins, S. Fateixa, T. Fernandes, H.I.S. Nogueira, T. Trindade, Inkjet printing of Ag and polystyrene nanoparticle emulsions for the one-step fabrication of hydrophobic paper-based surface-enhanced Raman scattering substrates, ACS Appl. Nano Mater. 4 (5) (2021) 4484–4495, https://doi.org/10.1021/acsanm.1c00112.

[30] C.C. Wu, F. Li, F. Lv, P. Yao, M.H. Bi, T. Xue, Fabrication of hydrogels with nanoparticles as surface-enhanced Raman scattered (SERS) substrates and their application in Raman imaging, Mater. Res. Express 8 (1) (2021) 015008, https://doi.org/10.1088/2053-1591/abd5d0.

[31] T.N.Q. Trang, L.Q. Vinh, T.T. Doanh, V.T.H. Thu, Structure-adjustable colloidal silver nanoparticles on polymers grafted cellulose paper-based highly sensitive and selective SERS sensing platform with analyte enrichment function, J. Alloy. Compd. 867 (2021) 159158, https://doi.org/10.1016/j.jallcom.2021.159158.

[32] S. Fateixa, H.I.S. Nogueira, T. Trindade, Surface-enhanced Raman scattering spectral imaging for the attomolar range detection of crystal violet in contaminated water, ACS Omega 3 (4) (2018) 4331–4341, https://doi.org/10.1021/acsomega.7b01983.

[33] J.C. Wang, G.B. Yi, Flexible and superhydrophobic silver nanoparticles decorated aligned silver nanowires films as surface-enhanced Raman scattering substrates, Nanoscale Res. Lett. 14 (2019) 292, https://doi.org/10.1186/s11671-019-3117-5.

[34] P. Pandey, S. Vongphachanh, J. Yoon, B. Kim, C.J. Choi, J.I. Sohn, W.K. Hong, Silver nanowire-network-film-coated soft substrates with wrinkled surfaces for use as stretchable surface enhanced Raman scattering sensors, J. Alloy Compd. 859 (2021) 157862, https://doi.org/10.1016/j.jallcom.2020.157862.

[35] S.Y. Chen, Q. Li, D. Tian, P. Ke, X.X. Yang, Q.Y. Wu, J. Chen, C.L. Hu, H.B. Ji, Assembly of long silver nanowires into highly aligned structure to achieve uniform "Hot Spots" for Surface-enhanced Raman scattering detection, Spectrochim. Acta A 273 (2022) 121030, https://doi.org/10.1016/j.saa.2022.121030.

[36] J.J. Luo, Z.K. Wang, Y. Li, C.D. Wang, J.F. Sun, W.C. Ye, X.L. Wang, B. Shao, Durable and flexible Ag-nanowire-embedded PDMS films for the recyclable swabbing detection of malachite green residue in fruits and fingerprints, Sensor. Actuat. B-Chem. 347 (2021) 130602, https://doi.org/10.1016/j.snb.2021.130602.

[37] G.D. Xu, N. Li, Y. Sun, C. Gao, L.P. Ma, P. Song, L.X. Xia, A label-free, rapid, sensitive and selective technique for detection of Fe^{2+} using SERRS with 2,2'-bipyridine as a probe, Chem. Eng. J. 414 (2021) 128741, https://doi.org/10.1016/j.cej.2021.128741.

[38] K. Siskova, O. Becicka, K. Safarova, R. Zboril, HCl effect on two types of Ag nanoparticles utilizable in detection of low concentrations of organic species, ACS Symp. Ser. 1124 (2013) 151–163, https://doi.org/10.1021/bk-2013-1124.ch009.

[39] E.B. Kaganovich, I.M. Krischenko, S.A. Kravchenko, E.G. Manoilov, B. O. Golichenko, A.F. Kolomys, V.V. Strel'chuk, SERS spectroscopy of nanocomposite porous films containing silver nanoparticles, Opt. Spectrosc. 118 (2) (2015) 294–299, https://doi.org/10.1134/S0030400X15020071.

[40] Z.X. Luo, B.H. Loo, X.Q. Cao, A.D. Peng, J.N. Yao, Probing the conformational transition of 2, 2'-bipyridyl under external field by surface-enhanced Raman spectroscopy, J. Phy. Chem. 116 (4) (2012) 2884–2890, https://doi.org/10.1021/jp208566d.